Analysis of Over-the-Air Time Synchronization for Industrial LiFi Networks

Ahmet Burak Ozyurt and Wasiu O. Popoola
Institute for Digital Communications, School of Engineering, The University of Edinburgh, EH9 3JL, Edinburgh, UK. Email:{a.b.ozyurt, w.popoola}@ed.ac.uk

***Abstract*—This paper analyzes a new and accurate over-the-air time synchronization (TS) method for industrial LiFi networks which achieves synchronization via the exchange of timestamps between nodes. The necessity for accurate TS will become increasingly important with future networks due to its connection with industrial applications. Over-the-air TS vision is to achieve accuracy of the order of $1\ \mu$s. In this technique, timestamps are transmitted using optical signals which are used for the estimation of the time-of-arrival (TOA). To this end, the Cramer-Rao Lower Bound (CRLB) is computed as the theoretical limit on the performance and accuracy. In this way, the effects of distance, optical power, and semi-angle at half illuminance of the transmitter are investigated. Calculations and comparison show that the proposed technique can be efficiently used for TS in future wireless networks.**

***Keywords*—Time synchronization, LiFi, industrial networks.**

I. INTRODUCTION

While the commercial deployment of 5G and WiFi 6 is still in its early stage, planning and research for future networks has already started. New use cases, such as high-precision manufacturing and full automated driving, with tighter communication requirements need to be addressed in future networks [1]. In this paper, we select to focus on an important part of future networks which is time synchronization (TS) [2]. In particular, we propose the use of optical wireless signals (LiFi) as a means of achieving an accuracy of the order of $1\ \mu$s, as envisioned by 5GPPP [3].

TS is defined as the exchange of timestamps between the network nodes. In the general case, a master node broadcasts timestamps to the involved slave nodes. Regarding the strict TS target of future networks, it is clear that new techniques and enablers are required for reaching a more precise TS. As shown in [2], the main constraint for more accurate over-the-air TS is the uncertainty imposed by the propagation of the radio frequency (RF) signals. This uncertainty can reach up to ± 100 ns. In particular, TS using RF signal becomes challenging due to:

- perturbation of the true time of arrival (TOA) due to noise and line-of-sight (LoS)/non-LoS (NLoS) multi-path propagation [4].
- the wide bandwidth requirements [5].
- susceptibility to malicious RF jamming from neighboring transmitters [5].
- high implementation cost of the required complex circuitry (front-ends, mixers, etc).

Thus, the tight TS requirements of future networks in conjunction with the above challenges motivate the use of optical signal based LiFi technology for over-the-air TS between master and slave nodes. The main differences between such configuration from conventional methods are as follows. The optical wireless channel is more directional, with less, and in many setups negligible multi-path propagation, and without small scale fading. These characteristics of the optical wireless channel ensure the deterministic attenuation of the transmitted optical signal [6]. In synchronization with LiFi, the front ends of the transceiver are relatively simple and cheap devices. In particular, they operate in the baseband and do not require frequency mixers or sophisticated algorithms for the compensation impairments, such as phase noise and IQ imbalances, which are present in RF communication [7]. Light transmitters are energy-efficient sources and their use enables higher energy efficiency [7]. Moreover, the optical spectrum is unlicensed with limited use for communication currently. As light does not travel through opaque objects, LiFi offers physical layer security advantages when compared to radio waves. Furthermore, in indoor deployments, external jamming is difficult or even impossible in the LiFi TS system. This is particularly important in industrial use case. Finally, optical-based TS can be easily adapted to existing TS standards.

In order to provide satisfactory quality of service, future networks need to further enhance TS by embracing novel methods. Especially, high-precision manufacturing, fully automated driving, power distribution, and wireless live audio/video production appear as potential use cases for optical-based TS systems. First, the real-time control command is transmitted over-the-air links between the controller and devices. Because propagation is mostly via the LoS and the bandwidth is high for optical bands, optical-based TS is perfectly suitable for a high-precision manufacturing environment. Second, with the introduction of fully automated driving, ensuring timely and robust delivery of safety-related messages takes a critical place which is related to precise TS. Moreover, power plants are very RF-sensitive and optical networks are proposed to ensure risk-free operations. Power plants require precise TS for fault location, control, optimization, monitoring, and diagnostics. Professional media content requires capturing samples at different devices at precisely the same point in time. Considering that LiFi is known as a low-latency communication enabler without

This work is funded by the European Union's Horizon 2020 research and innovation programme under the Marie Skłodowska Curie grant agreement No. 814215 titled ENLIGHT'EM: European Training Network in Low-Energy Visible Light IoT Systems: https://enlightem.eu/.

For the purpose of open access, the authors have applied a Creative Commons Attribution (CC BY) licence to any Author Accepted Manuscript version arising from this submission.

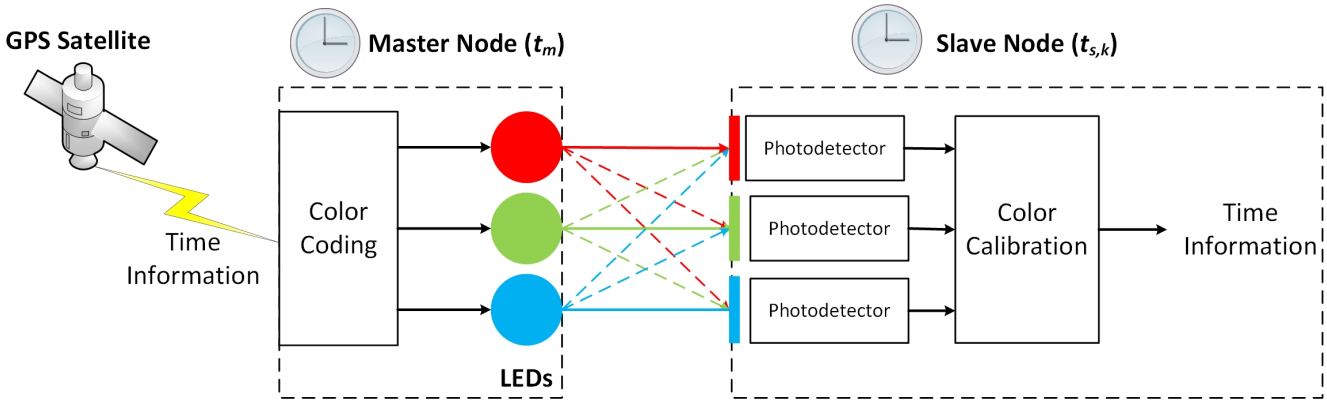

Fig. 1: An architecture of the optical-based time synchronization distribution with a master node, slave node and a GPS satellite as a time source.

jitter in indoor scenarios, optical-based TS emerges as an optimal solution for wireless A/V production [8].

The foregoing provides a motivation to investigate TS in the optical band (infrared and visible light) as a new and promising technique for next-generation networks. The previous synchronization studies in the optical bands are mostly about the modulation schemes such as orthogonal frequency division multiplexing (OFDM) and direct current biased optical OFDM (DCO-OFDM). However, obtained results are directly related to physical layer enhancement which is out of the scope of this study. A few system-level synchronization studies, which are relevant to this paper, are reported in the optical bands. In [9], a design that combines visible light communication (VLC) and RF backscatter into a self-powered autonomous circuit is given for frequency synchronization, not for TS. In [10], a time synchronization method is proposed using non-line-of-sight VLC to synchronize all the transmitters that will form a beamspot to serve the same receiver. That is, synchronization among identical transmitters on the ceiling not between transmitters and receivers. This study is based on experimental measurements, so it does not provide an analytical framework. Besides, when it is considered that the reflected signals for VLC/LiFi are very weak and only account for less than 3% of the total received power, the obtained results do not show the real potential of TS in the optical bands [11]. To the authors' best knowledge, over-the-air TS with LiFi networks between transmitters and receivers which operate in the visible or infrared bands does not exist in the previous works except our published patent file [12].

In this paper, we propose and explore the accuracy of TS using optical signals. The major contributions of this paper are summarized as follows: 1) showing that over-the-air optical-based TS method is a promising solution for future networks; 2) the TOA of optical signals is characterized via the derivation of its Cramer-Rao Lower Bound (CRLB); 3) a closed-form expression is derived and studied using numerical results. This is done by taking into account the most important system parameters.

II. SYSTEM MODEL AND BASIC ASSUMPTIONS

The system model of the considered optical-based TS technique is given in Figure 1. In this scenario, optical-based TS can serve as a complementary solution to the conventional RF TS or as a stand-alone solution. In an optical system, a number of LEDs are transmitting optical signals. In the receiver side, a number of PDs are used for the collection of the impinging optical power. In TS, the transmitted optical signal represents the reference clock of the master node. In this paper, we assume that the clock of the master node is aligned with the clock of the Global Positioning Systems (GPS).

TS refers to the overall mechanism of keeping multiple clocks synchronized with the reference clock. In particular, in a TS system, one device acts as a master node which maintains a master clock, t_m. The other devices, termed as slave nodes, aim to align their clocks to the clock of the master node. The clock time, $t_{s,k}$, of the k-th slave node relies on the master clock to correct its timing. In this paper, the reference source of time from the master node, t_m, to the k-th slave node, $t_{s,k}$, is distributed with LiFi signals. Furthermore, TS is achieved with the exchange of timestamps encoded in optical signals which are independent of modulation techniques. The coding scheme can be implemented with specific modulation formats, such as color shift keying (CSK), pulse amplitude modulation (PAM), or optical orthogonal frequency division multiplexing (OFDM) [6]. An alternative approach is to represent a timestamp directly using one particular combination of shades of color. In this case, the color-based coding scheme is implemented using a predefined color codebook according to which different timestamps are encoded by different shades of color.

In LiFi networks, there are two types of background noise which are the sunlight and the light noise from illumination fixtures. In both cases, these types of noise result in: i) the addition of DC component to the received optical signal and ii) an insignificant increase of the ambient noise. Consequently, their effect can be easily mitigated in the optical-based TS or in any other LiFi deployment. Furthermore, it should be emphasized that this idea is mostly envisaged for indoor industrial applications where the environment

is controlled and carefully designed. In addition, industrial spaces are usually closed with minimum windowing or even with no windowing.

Another factor that could distort the permanence of LiFi based TS is optical interference from the surrounding LiFi communication infrastructure. However, for LiFi based TS, just like most of the existing RF TS standards, it can be assumed that there is a temporal or frequency separation between the resources allocated for communication and TS.

Other important factors that need to be considered in LiFi based TS include blockage of the propagation path and the mobility of any participating devices. For both cases, a solution can be found by deploying an internal clock in all slave nodes which can be used in case of of disturbance of the LiFi based TS. The TS information can be kept by the system's internal clock in long term (holdover time); thus, continuous communication is not necessary for TS like other types of data transmission.

In more detail, the transmitted timestamps are represented as different points of a given color representation scheme. For example, in an RGB LED color representation scheme, timestamps are represented as different shades of red, green, and blue. However, modelling such a coding scheme is outside the scope of the work. In this way, a precise synchronization can be achieved without experiencing some of the challenges in the RF spectrum such as multipath fading and inter-layer interference. The general technique for updating TS information is conducted from a master clock to a slave clock as $t_{s,k} \leftarrow t_m$.

In LiFi networks, especially in industrial setups, the effect of multiple reflections from the objects and human shadowing is ignored [11]. This means that only LoS is taken into account for the LiFi channel model used in this study. According to this assumption, the channel gain of LiFi system can be expressed as [6]:

$$\eta_{\mathrm{LOS}}(d) = \frac{(m+1)A_r}{2\pi d^2}\cos^m(\varphi)T_s g(\psi)\cos(\psi), \qquad (1)$$

where d is the distance between the receiver and transmitter, A_r is the receiver effective area, ψ is the angle of incidence with respect to the axis normal to the receiver surface, φ is the angle of irradiance with respect to the axis normal to the transmitter surface, ψ_{con} is the field-of-view (FOV), $g(\psi)$ is the concentrator gain, T_s is the filter transmission, respectively, and m is the Lambertian index described as [6]:

$$m = -\frac{\ln(2)}{\ln[\cos(\varphi_{1/2})]}. \qquad (2)$$

Here, $\varphi_{1/2}$ is the semi-angle at half illuminance of the transmitter. Also, the gain of the optical concentrator at the receiver is expressed by [6]:

$$g(\psi) = \begin{cases} n^2/\sin^2(\psi_{con}), & \text{if } 0 < \psi \leq \psi_{con} \\ 0, & \text{if } \psi_{con} \leq \psi, \end{cases} \qquad (3)$$

where n is the refractive index.

For simplicity, we assume that $g(\psi) = T_s = 1$ and that the transmitter and receiver are aligned such as in Figure 1. Thus, the received power at the receiver is given as [6]:

$$x = R_p \eta_{LOS} P_t + w = P_0 + w \qquad (4)$$

where $P_0 = R_p \frac{(m+1)A_r}{2\pi d^2}\cos^m(\varphi)T_s g(\psi)\cos(\psi)P_t$, w is zero-mean additive white Gaussian noise (AWGN), R_p is photodiode responsivity and P_t is transmitted optical power.

In a LiFi system, the total noise can be given as:

$$\sigma_0^2 = \sigma_t^2 + \sigma_s^2 \qquad (5)$$

where σ_t^2 symbolizes the thermal noise variance which is constant and independent of the optical power. While, σ_s^2 denotes the shot noise variance which depends on the received optical power. The shot and thermal noise variances are defined as, $\sigma_t^2 = \frac{8\pi\kappa T_k}{G_{ol}} C_{pd} A_r I_2 B^2 + \frac{16\pi^2 \kappa T_k \Gamma}{g_m} C_{pd}^2 A_r^2 I_3 B^3$, and, $\sigma_s^2 = 2qB(P_0 + I_B I_2)$, respectively, where, the bandwidth of the electrical filter that follows the photodetector is represented by B Hz, κ is the Boltzmann's constant, I_B is the photocurrent due to background radiation, T_k is absolute temperature, G_{ol} is the open-loop voltage gain, C_{pd} is the fixed capacitance of photodetector per unit area, Γ is the FET channel noise factor, g_m is the FET transconductance and noise-bandwidth factors, I_2 = 0.562, and I_3 = 0.0868 [6].

III. CRAMER-RAO LOWER BOUND FOR OPTICAL-BASED TIME SYNCHRONIZATION

The precision clock synchronization protocol of the IEEE 1588 standard defines TS as a set of periodic message exchanges which is used to capture the propagation delay of the network and thus calculate the time offset between master and slave nodes that are geographically separated across links/nodes. In TS, the propagation delay is measured using the time-of-arrival (TOA) parameter. The TOA, τ, between the transmitter and receiver of interest can be inferred from their distance, d, as $d = c\tau$, where c is the speed of light [13]. Due to jitter which exists because of thermal noise in the electrical circuits and inter-symbol interference, the measurement of the TOA from the receiving node needs to be characterized statistically.

The measure of goodness usually consists of the variance; that is, the word "best" is interpreted to mean the smallest variance about the true parameter value. It is possible to derive an expression for the smallest possible variances in terms of effective measures of such waveform parameters as the bandwidth and the time duration. An efficient estimator provides the smallest error variance. In this paper, an estimator, $\hat{\tau}$, of the actual TOA, τ, is derived by leveraging the form of the received optical signal given by (4). This is done by evaluate the CRLB which is defined as the lower bound of the variance of an unbiased estimator of an unknown parameter [14]. Focusing on a point-to-point optical link, (4) reveals that the received optical signal can be described as a Gaussian random variable (RV), with variance, σ_0^2, and mean value, P_0. Thus, its probability density function (pdf) is given as [15]:

$$f(x;\hat{\tau}) = \frac{1}{\sqrt{2\pi}\sigma_0}\exp\left\{-\frac{1}{2\sigma_0^2}(x-P_0)^2\right\}. \qquad (6)$$

From (6), we can obtain using the the natural logarithm that:

$$\ln f(x;\hat{\tau}) = -\ln\sqrt{2\pi}\sigma_0 - \frac{1}{2\sigma_0^2}(x-P_0)^2. \qquad (7)$$

Considering that, $P_0 = R_p \frac{(m+1)A_r}{2\pi d^2}\cos^m(\varphi)T_s g(\psi)\cos(\psi)P_t$ from (4) and that $d = c\hat{\tau}$, the first order derivative of (7)

$$\frac{\partial^2 \ln f(x;\hat{\tau})}{\partial \hat{\tau}^2} = \frac{2(qB)^2}{\sigma_0^4}\left(\frac{\partial P_0}{\partial \hat{\tau}}\right)^2 - \frac{qB}{\sigma_0^2}\frac{\partial^2 P_0}{\partial \hat{\tau}^2} - \frac{4(qB)^2}{\sigma_0^6}(x-P_0)^2\left(\frac{\partial P_0}{\partial \hat{\tau}}\right)^2 - \frac{2qB}{\sigma_0^4}(x-P_0)\left(\frac{\partial P_0}{\partial \hat{\tau}}\right)^2 + \frac{qB}{\sigma_0^4}(x-P_0)^2\frac{\partial^2 P_0}{\partial \hat{\tau}^2} - \frac{2qB}{\sigma_0^4}(x-P_0)\left(\frac{\partial P_0}{\partial \hat{\tau}}\right)^2 - \frac{1}{\sigma_0^2}\left(\frac{\partial P_0}{\partial \hat{\tau}}\right)^2 + \frac{1}{\sigma_0^2}(x-P_0)\frac{\partial^2 P_0}{\partial \hat{\tau}^2}. \tag{11}$$

with respect to $\hat{\tau}$ is given as:

$$\frac{\partial \ln f(x;\hat{\tau})}{\partial \hat{\tau}} = -\frac{\frac{\partial \sigma_0}{\partial \hat{\tau}}}{\sigma_0} + \frac{\frac{\partial \sigma_0}{\partial \hat{\tau}}}{\sigma_0^3}(x-P_0)^2 + \frac{1}{\sigma_0^2}(x-P_0)\frac{\partial P_0}{\partial \hat{\tau}}. \tag{8}$$

The relationship between the total noise from (5) and estimated TOA is equal to:

$$\frac{\partial \sigma_0}{\partial \hat{\tau}} = \left[\sigma_t^2 + 2qBP_0 + 2qBI_BI_2\right]^{-0.5} qB\frac{\partial P_0}{\partial \hat{\tau}} = \frac{qB}{\sigma_0}\frac{\partial P_0}{\partial \hat{\tau}}. \tag{9}$$

The total noise in (9), σ_0^2, includes the shot noise variance, σ_s^2, in (5). Also, P_0 is a contributor to the shot noise variance and is directly related to estimator $\hat{\tau}$ like in (7). Combining (8) and (9) gives:

$$\frac{\partial \ln f(x;\hat{\tau})}{\partial \hat{\tau}} = -\frac{qB}{\sigma_0^2}\frac{\partial P_0}{\partial \hat{\tau}} + \frac{qB}{\sigma_0^4}(x-P_0)^2\frac{\partial P_0}{\partial \hat{\tau}} + \frac{1}{\sigma_0^2}(x-P_0)\frac{\partial P_0}{\partial \hat{\tau}}. \tag{10}$$

In order to find the CRLB of the TOA, the second derivative of (7) is required. The result of this is given in (11). Upon taking the negative expected value of (11), we have that:

$$-\mathbf{E}\left[\frac{\partial^2 \ln f(x;\hat{\tau})}{\partial \hat{\tau}^2}\right] = \left(\frac{\partial P_0}{\partial \hat{\tau}}\right)^2\left[\frac{1}{\sigma_0^2} - \frac{2(qB)^2}{\sigma_0^4}\right]. \tag{12}$$

Then, the CRLB for TOA can be given as:

$$\sqrt{var(\hat{\tau})} \geq \frac{\sigma_0^2}{\left|\frac{\partial P_0}{\partial \hat{\tau}}\right|}\sqrt{\frac{1}{\sigma_0^2 - 2q^2B^2}} \tag{13}$$

where value of $\frac{\partial P_0}{\partial \hat{\tau}}$ given by:

$$\frac{\partial P_0}{\partial \hat{\tau}} = -\frac{(m+1)A_r c}{\pi d^3}R_p P_t. \tag{14}$$

As can be seen from (13) and (14), the CRLB of the estimator of the TOA becomes more precise with the increase of the receiver effective area, photodiode responsivity, and optical power. In contrast, its accuracy degrades with the distance and semi-angle at half illuminance of the transmitter.

IV. NUMERICAL RESULTS AND DISCUSSION

In this section, the numerical evaluation of the proposed optical-based TS technique is presented. The behavior of the provided estimator, $\hat{\tau}$, is characterized in terms of transmission distance, d, transmitted optical power, P_t, semi-angle at half illuminance of the transmitter, $\varphi_{1/2}$, using the CRLB given in (13). Table I presents the system setup considered in this section.

In order to highlight that the smaller values of CRLB variance provide a more accurate TOA estimation, in Figure 2, the value of the CRLB, as given in (13), is evaluated with respect the semi-angle at half illuminance of the transmitter, $\varphi_{1/2}$, for a distance of $d = 5$ m. As shown in Figure 2, the CRLB decreases as the transmitted optical power increases.

Table I: Simulation Parameters

Parameter	**Value**
Photodiode Responsivity (R_p)	0.4 mA/mW
Fixed Capacitance of PD (C_{pd})	112 pF/cm^2
Electron Charge (q)	1.6 $\times 10^{-19} C$
Channel Noise Factor(Γ)	1.5
Equivalent Noise Bandwidth (B)	400 MHz
Open-Loop Voltage Gain (G_{ol})	10
Absolute Temperature (T_k)	300 K
Receiver Effective Area (A_r)	1 cm^2
Light Speed (c)	299792458 m/s
Background Radiation (I_B)	0.04 A
Transconductance (g_m)	30 ms
Boltzmann's Constant (κ)	1.38 $\times 10^{-23}$

This is due to the higher receive SNR. On the other hand, the CRLB of the TOA increases as the semi-angle half illuminance, $\varphi_{1/2}$, increases. In fact, despite the point that a larger semi-angle at half illuminance, $\varphi_{1/2}$, provides a wider coverage area, the transmitted power is spread over a much wider area than the receiver active area. Thus, the collected optical power is reduced.

Next, we study the effect of distance, d, and transmitted optical power, P_t, on CRLB of TOA. In Figure 3, for several values of transmitted optical power, P_t, the CRLB is plotted against the distance between transmitter and receiver for $\varphi_{1/2} = 60^o$. Obviously by increasing the distance, the CRLB increases. In addition, it can be concluded that the CRLB decreases with higher transmitted power, P_t.

In order to observe the relations between the optical-based and conventional RF-based techniques for TOA es-

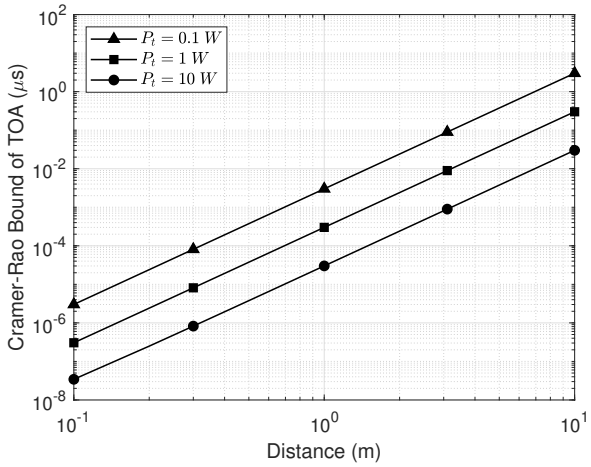

Fig. 2: The CRLB of TOA performance against the distance for different transmitted optical power at $\varphi_{1/2} = 60^o$.

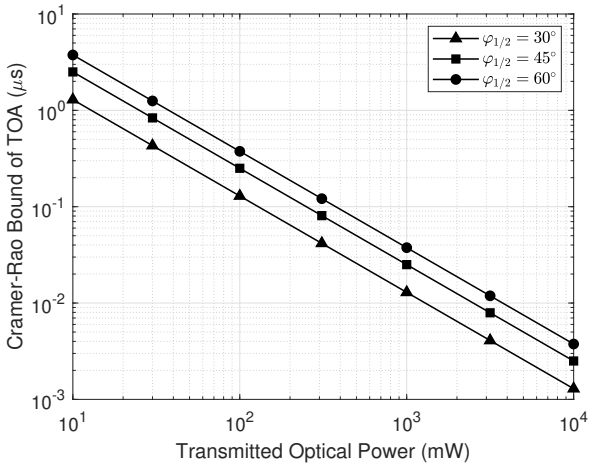

Fig. 3: The CRLB of TOA performance against the source optical power for different semi-angle at half illuminance of the transmitter at $d = 5$ m.

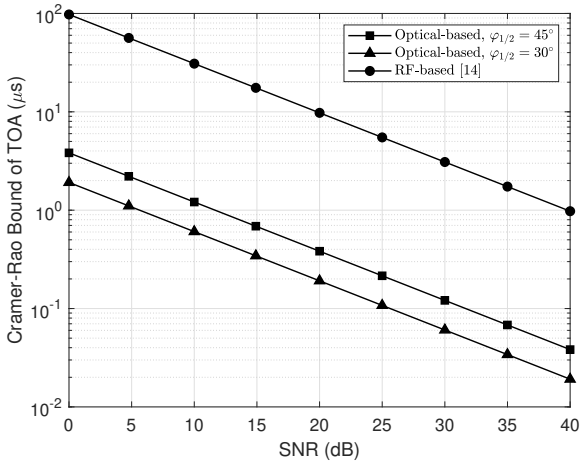

Fig. 4: The TOA performance of proposed optical-based and conventional RF-based technique against the SNR for different semi-angle at half illuminance of the transmitter at $d = 5$ m. [14].

timation, the CRLB of TOA is compared with the derived expression in [14]. In Figure 4, the CRLB of the optical-based technique is shown against the different signal-to-noise ratio (SNR $= P_0^2/\sigma_0^2$) values for different semi-angle at half illuminance of the transmitter at $d = 5$ m. The figure shows that the CRLB of TOA getting more precise for both techniques with increasing SNR. More importantly, this figure shows that CRLB of TOA for optical-based technique has better precision than the conventional RF-based technique as expected because of the deterministic and accurate nature of optical-based TS.

It is also to be highlighted that this paper is a preliminary work for over-the-air TS within visible/infrared band communication. Thus, a suitable algorithmic approach for optical-based TS, or a coding scheme will be the subject of further studies. The obtained results show that the optical-based method has potential for TS in future networks and is worth investigating deeper.

V. CONCLUSION

In this paper, we propose a optical-based TS technique which could be used as a stand-alone solution for TS or as a complementary RF TS. In the proposed solution, a master node transmits the timestamp to a number of slave nodes using LiFi signals. The performance of LiFi based TS is evaluated using the CRLB of TOA. The effect of distance, optical power, and Lambertian index on the performance of proposed TS method is characterized. Based on the preliminary results, it is concluded that LiFi based TS is a good candidate for future TS standards.

REFERENCES

[1] Z. Zhang, Y. Xiao, Z. Ma, M. Xiao, Z. Ding, X. Lei, G. K. Karagiannidis, and P. Fan, "6G wireless networks: Vision, requirements, architecture, and key technologies," *IEEE Vehicular Technology Magazine*, vol. 14, no. 3, pp. 28–41, 2019.

[2] A. Mahmood, M. I. Ashraf, M. Gidlund, J. Torsner, and J. Sachs, "Time synchronization in 5G wireless edge: Requirements and solutions for critical-mtc," *IEEE Communications Magazine*, vol. 57, no. 12, pp. 45–51, 2019.

[3] J. Cosmas, N. Jawad, M. Salih, S. Redana, and O. Bulakci, "5GPPP architecture working group view on 5G architecture: Version 4.0," 2021.

[4] H. Li, L. Han, R. Duan, and G. M. Garner, "Analysis of the synchronization requirements of 5G and corresponding solutions," *IEEE Communications Standards Magazine*, vol. 1, no. 1, pp. 52–58, 2017.

[5] A. Boukerche and D. Turgut, "Secure time synchronization protocols for wireless sensor networks," *IEEE Wireless Communications*, vol. 14, no. 5, pp. 64–69, 2007.

[6] Z. Ghassemlooy, W. Popoola, and S. Rajbhandari, *Optical wireless communications: system and channel modelling with Matlab®*. CRC press, 2019.

[7] P. H. Pathak, X. Feng, P. Hu, and P. Mohapatra, "Visible light communication, networking, and sensing: A survey, potential and challenges," *IEEE Communications Surveys Tutorials*, vol. 17, no. 4, pp. 2047–2077, 2015.

[8] J. Pilz, B. Holfeld, A. Schmidt, and K. Septinus, "Professional live audio production: A highly synchronized use case for 5G urllc systems," *IEEE Network*, vol. 32, no. 2, pp. 85–91, 2018.

[9] A. Torrisi, K. S. Yıldırım, and D. Brunelli, "Autonomous energy status sharing and synchronization for batteryless sensor networks," in *Proceedings of the 19th ACM Conference on Embedded Networked Sensor Systems*, 2021, pp. 569–571.

[10] J. Beysens, Q. Wang, A. Galisteo, D. Giustiniano, and S. Pollin, "A cell-free networking system with visible light," *IEEE/ACM Transactions on Networking*, vol. 28, no. 2, pp. 461–476, 2020.

[11] C. Chen, D. A. Basnayaka, and H. Haas, "Downlink performance of optical attocell networks," *Journal of Lightwave Technology*, vol. 34, no. 1, pp. 137–156, 2016.

[12] A. B. Ozyurt, A. Stavridis, and Y. Turk, "Technique for performing time synchronization," *WIPO, WO/2022/117234*, Jun 2022.

[13] T. Q. Wang, Y. A. Sekercioglu, A. Neild, and J. Armstrong, "Position accuracy of time-of-arrival based ranging using visible light with application in indoor localization systems," *Journal of Lightwave Technology*, vol. 31, no. 20, pp. 3302–3308, 2013.

[14] H. V. Poor, *An introduction to signal detection and estimation*. Springer Science & Business Media, pp. 102-120, 2013.

[15] C. Amini, P. Azmi, and S. S. Kashef, "Theoretical accuracy analysis of RSS-based range estimation for visible light communication," *arXiv preprint arXiv:2011.14080*, 2020.